

# Analysis of Microstructural Textures and Wave Propagation Characteristics in Shales

Manika Prasad\* and Tapan Mukerji  
Stanford Rock Physics Laboratory.

## Summary

We apply different statistical methods for characterizing heterogeneity and textures from scanning acoustic microscope (SAM) images of shale microstructures. Characterizing and understanding the microgeometry, their textures, scales, and textural anisotropy is important for better understanding the role of microgeometry on effective elastic properties. We analyzed SAM images from Bakken shale, Bazhenov shale, and Woodford shale. Our analysis, based on spatial autocorrelation functions shows that there is a small positive correlation between the degree of heterogeneity and the mean spatial correlation length of the microstructure. The textural anisotropy ranges from 10% to 80%. There is considerable variability within each image, as well as from one image to another. A singular value decomposition (SVD) spectral analysis showed that the shale microstructures have characteristics in common with fractal stochastic images. We also obtain a correlation between maturity and textural heterogeneity.

## Introduction

Microstructural characteristics of organic rich shales can give important insights on the maturation processes and on oil generation from such formations. Since changes in shale texture and in hydrogen content are closely linked with kerogen maturity, a correlation between them would enhance methods for detecting and prospecting of kerogen rich shales. The problem is complicated by the fact that the intrinsic anisotropic texture of the shales is enhanced by kerogen distribution in the shales. Attempts have been made to relate acoustic velocity and velocity anisotropy to the degree of kerogen maturity of the shales (Vernik and Nur, 1994; Vernik and Liu, 1997). These studies have been instrumental in improving our understanding of the ultrasonic properties in kerogen rich shales. We have revisited the ultrasonic data collected by Vernik and co-authors and interpreted them using recent acoustic microscopy analyses of the impedance microstructure of the shales (Prasad and Nur, 2001)

Optical and scanning electron microscopy methods to analyze kerogen shale microstructure have been utilized in the past. However, due to the opaque nature of the kerogen and the associated pyrite, such methods are rather difficult to implement. In addition to optical and scanning electron microscopy, we used a non-destructive technique to map the impedance microstructure of kerogen-rich shales with a scanning acoustic microscope. With this technique we were able to map changes in elastic properties as the shales

undergo maturation. This paper reports results of acoustic characterization in samples belonging to various maturity grades and with different kerogen contents. Image analyses techniques (described below) are used to detect changes in texture and heterogeneity in the acoustic microscopy images and are related to ultrasonic measurements.

## Statistical descriptions of heterogeneity and textures

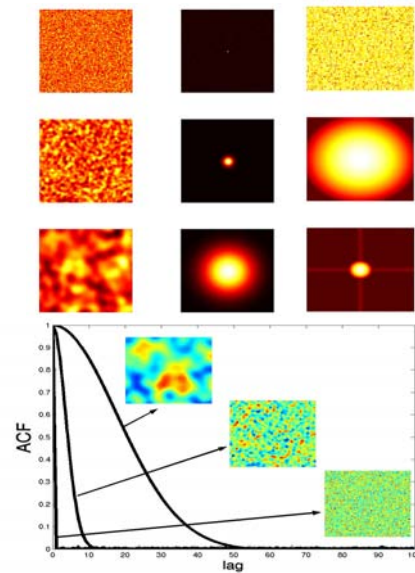


Figure 1: Spatial autocorrelation and spatial spectrum can be used to stochastically describe image textures and scales. Top left: Synthetic images with increasing spatial correlation; center: corresponding 2D autocorrelation function; right: corresponding 2D Fourier power spectra. Bottom: radial profiles of isotropic Gaussian autocorrelation functions showing the relation between textures and correlation length.

We used statistical descriptors to quantify the heterogeneity and textures observed in the images. The heterogeneity was quantified by the coefficient of variation (CV) given by the ratio of the standard deviation to the mean of the image pixel values. Gray scale image intensity values were converted to elastic impedances using a calibration function before computing their statistics. Textures can be quantified using spatial autocorrelation functions (Figure 1). We used Fourier transform based autocorrelation estimation. Radial profiles of the autocorrelation function along azimuths ranging from  $0^\circ$  to  $180^\circ$  were computed, and the correlation length estimated at each azimuth. The correlation length is taken to be the lag value where the correlation function

## Microstructural textures and anisotropy in Shales

falls to  $1/e$  of its maximum value at zero lag. The texture anisotropy was quantified by the anisotropy ratio (AR) defined as the ratio between the maximum and minimum correlation lengths obtained over all azimuths. Textures were also analyzed using a singular value decomposition (SVD) of the images. The spectrum of singular values shows different decay behavior for different textures (Figure 2).

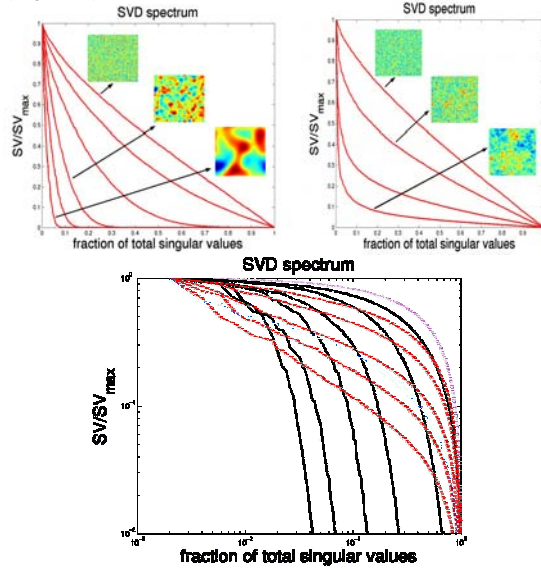


Figure 2: Singular value spectrum shows distinctive behavior for images with Gaussian spatial correlation (top left) versus fractal images (top right). In the bottom figure the black lines with a rapid fall off in singular value corresponds to images with Gaussian autocorrelation, while the dotted red lines correspond to SVD spectra of fractal images.

### SAM Images

Despite similar chemical compositions, microstructure of the samples differed considerably. Acoustic micrographs of the Bakken shale series samples, a Bazhenov shale and a Woodford shale are shown in Figure 3. The C-scan surface images were made at 1 GHz with a calibrated color scale. The calibrations were made using standard materials with known impedance (Prasad et al., 2002). From the different maturity shale samples examined in this study, we find following major differences in the impedance microstructural images:

- Increase in impedance as maturity progresses
- Increase in grain size and in the number of coarse grains in mature shales
- Kerogen and grain distribution undergo major change as the maturity progresses. In immature shale, kerogen forms a more or less connected matrix and the higher impedance grains are dispersed in this matrix. In more mature shale, there is a significant increase in number

of coarse grains. The grains appear to form a framework with kerogen globules distributed within this frame.

- Bedding parallel kerogen filled cracks appear to be more common in immature shale.

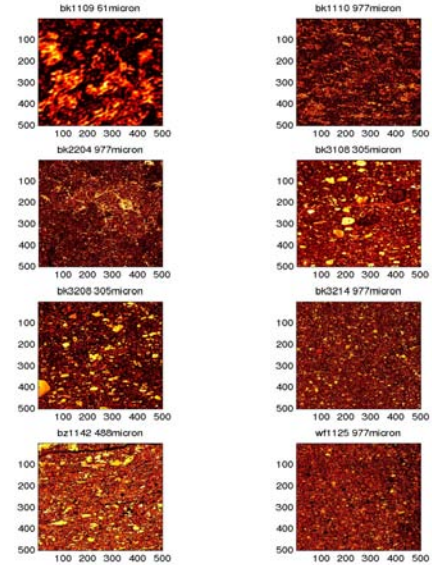


Figure 3: SAM images of Bakken shales (bk), Bazhenov shale (bz, lower left), and Woodford shale (wf, lower right). The images have differing resolutions. The image size in microns is indicated. The top left image has an order of magnitude higher resolution.

### Results of Image Analysis

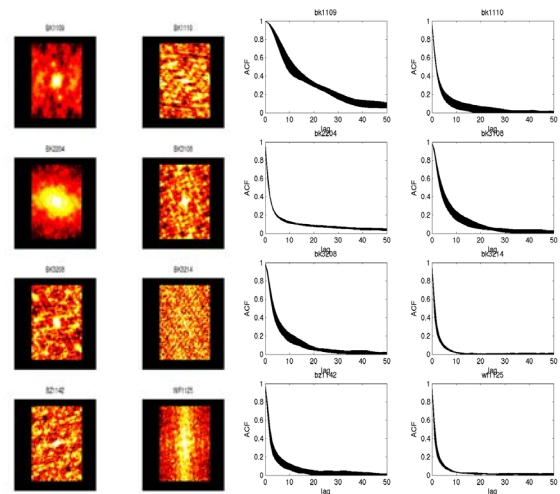


Figure 4: Left: 2-D spatial autocorrelation of the 8 SAM images in shown above in Figure 3. Right: Azimuthal profiles of the corresponding autocorrelation function from 0 to 180 degrees.

## Microstructural textures and anisotropy in Shales

The results of texture analyses are shown in Figures 4, 5, and 6. Figure 4 shows the estimated autocorrelation function and the azimuthal profiles. The impedance variation ranged from about 7% to 12%, while the mean correlation length ranged from 2 to 4.5 microns (Figure 5). In general the textural anisotropy (AR) increased with increasing heterogeneity (CV), as seen in Figure 6.

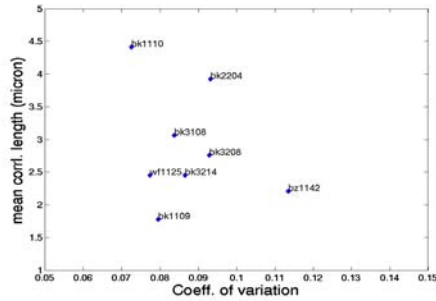


Figure 5: CV (heterogeneity) versus mean correlation length.

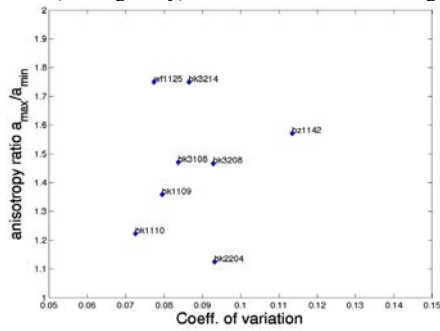


Figure 6: CV versus textural anisotropy. Textural anisotropy is measured by the ratio of maximum correlation length to the minimum correlation length.

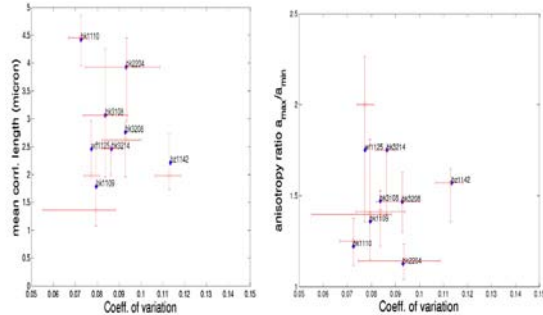


Figure 7: Variability with images. Bars indicate range of values obtained by sampling different subsections of the same image. Left: CV versus mean correlation length. Right: CV versus anisotropy ratio.

We analyzed variability within images by processing different subsections of the same image, making sure to sample subsections much larger than the mean correlation

length to obtain valid statistics. The variability is displayed in Figure 7. SVD spectra of the images are distinctly different from SVD spectra of synthetic images with Gaussian autocorrelation. They show more resemblance to SVD spectra of fractal images (Figure 8).

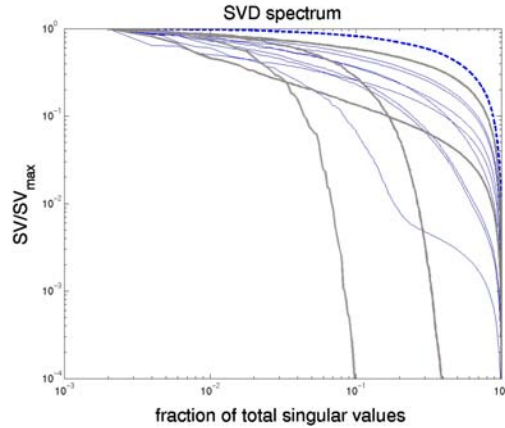


Figure 8: SVD spectra of all but one SAM image are similar to SVD spectra of fractal images showing a slower decay than SVD spectra of Gaussian images (compare with Figure 2). The curve with two humps, indicating two spatial scales comes from an image with an order of magnitude higher resolution. The dotted line is the SVD spectrum of a random image with no correlation.

### Summary of Acoustic Measurements

We reevaluated the ultrasonic and physical property data from Vernik and Landis (1987) to distinguish between effects of kerogen and porosity on the elastic properties. Figure 9 shows that porosity effects dominate velocity variations in high porosity shales. In low porosity shales, velocity correlates better with kerogen content (Figure 10).

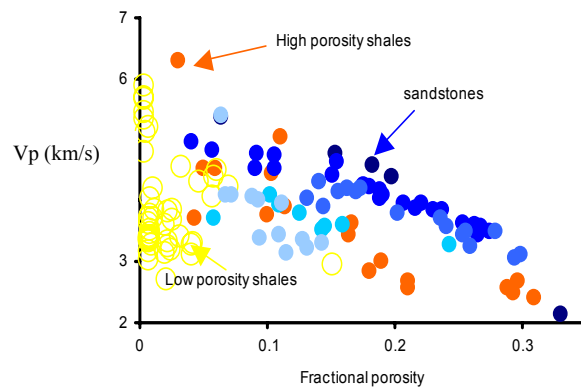


Figure 9: High-porosity kerogen shales resemble sandstones: There is a good correlation between  $V_p$  and porosity.

## Microstructural textures and anisotropy in Shales

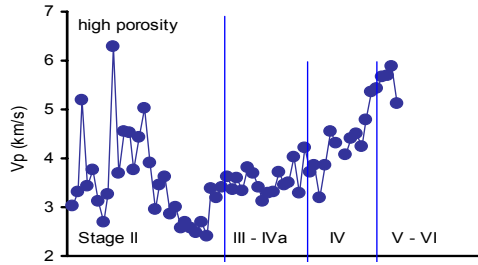


Figure 10: In low porosity kerogen shales, velocity increases with maturation.

### Textural and Acoustic Property Comparisons

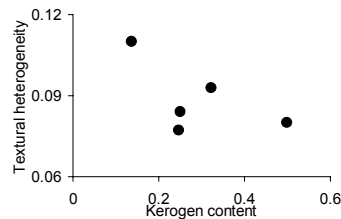


Figure 11: The coefficient of variation (CV) of impedance heterogeneity increases with maturity (decreasing kerogen content) implying an influx of stiffer materials in agreement with the observed increase in impedance with maturity.

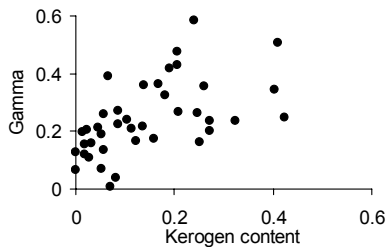


Figure 12: The ultrasonic velocity anisotropy (Thomsen's Gamma) is directly proportional to kerogen content: It decreases with decreasing kerogen content (increasing shale maturity)

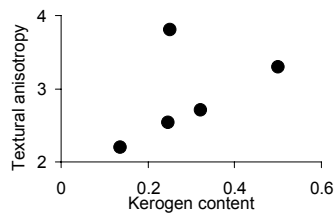


Figure 13: Similar to the anisotropy coefficient Gamma (Figure 12), spatial textural anisotropy ratio (AR) is also directly proportional to kerogen content. It decreases with maturity implying removal of aligned kerogen with maturity

Figure 11 shows the relation between maturity (decreasing kerogen content) and textural heterogeneity as quantified

by the CV. Increasing maturity is linked to increasing textural heterogeneity. At the same time, increasing maturity is linked to a general decrease in both ultrasonic velocity anisotropy measured by Thomsen's gamma parameter (Figure 12) as well as textural anisotropy measured by AR (Figure 13).

### Conclusions

Our analysis of SAM images shows the following: the coefficient of variation (CV), which is a measure of heterogeneity, ranges from 7% to about 12% for these shales. The spatial correlation length varies with direction, and the mean correlation length ranges from about 2 to 4.5 microns. There is a small positive dependence between the CV and the mean spatial correlation length. The mean correlation length generally tends to increase with increasing CV. The textural anisotropy, defined as the ratio of the maximum to minimum correlation length within an image, ranges from 20% to about 80% and in general tends to increase with increasing heterogeneity (CV). Singular value analysis of the images indicates that the SVD spectra of the shale microstructure tend to be similar to (but not exactly the same as) SVD spectra of fractal images. The textural heterogeneity (CV) increases with increasing maturity (decreasing kerogen content), while there is a general decrease in ultrasonic velocity anisotropy and textural anisotropy with maturity.

### Acknowledgements

We acknowledge the Stanford Rock Physics project, and support from U.S. DOE.

### References

- Prasad, M., Nur, A., 2001, Impedance Microstructure of Kerogen in Organic Rich Shales: AAPG Expanded Abstracts, Annual Convention, Denver.
- Prasad, M., Reinstaedler, M., Arnold, W., 2002, Quantitative acoustic microscopy: Applications to petrophysical studies of reservoir rocks: Acoustical Imaging 25, Kluwer Publications.
- Vernik, L. and Landis, C., 1996, Elastic anisotropy of source rocks: Implications for hydrocarbon generation and primary migration: AAPG Bull., 80, 531 – 544.
- Vernik, L. and Liu, X., 1997, Velocity anisotropy in shales: A petrophysical study: Geophysics, 62, no. 2, 521 – 532.
- Vernik L. and Nur, 1994; Ultrasonic velocity and anisotropy of hydrocarbon source rocks: Geophysics, 57, no. 5, 727 – 7351.